

Sampling reduced density matrix to extract fine levels of entanglement spectrum

Bin-Bin Mao,¹ Yi-Ming Ding,² and Zheng Yan^{2,3,*}

¹*School of Foundational Education, University of Health and Rehabilitation Sciences, Qingdao 266000, China*

²*Department of Physics, School of Science, Westlake University, Hangzhou 310030, China*

³*Institute of Natural Sciences, Westlake Institute for Advanced Study, Hangzhou 310024, China*

Low-lying entanglement spectrum provides the quintessential fingerprint to identify the highly entangled quantum matter with topological and conformal field-theoretical properties. However, when the entangling region acquires long boundary with the environment, such as that between long coupled chains or in two or higher dimensions, there unfortunately exists no universal yet practical method to compute the entanglement spectra with affordable computational cost. Here we propose a new scheme to overcome such difficulty and successfully extract the low-lying fine entanglement spectrum (ES). We trace out the environment via quantum Monte Carlo simulation and diagonalize the reduced density matrix to gain the ES. We demonstrate the strength and reliability of our method through long coupled spin chains and answer its previous controversy. In addition, 2D examples have also been displayed which reveal the continuous symmetry breaking phase through a tower of states ES. Our simulation results, with unprecedentedly large system sizes, establish the practical computation scheme of the entanglement spectrum with a huge freedom degree of environment.

Introduction.- Quantum informatics and condensed matter physics have been increasingly cross-fertilizing each other in recent years [1, 2]. Within this trend, quantum entanglement was proposed to detect the field-theoretical and topological properties of quantum many-body systems [3–6]. For example, it usually offers the direct connection to the conformal field theory (CFT) and categorical description [7–17]. Beyond the entanglement entropy (EE), Li and Haldane proposed that the entanglement spectrum (ES) is a more fundamental entanglement characteristic to quantify the intrinsic information of many-body systems [18–22]. They also suggested a profound correspondence between the ES of an entangled region with the energy spectra on the related virtual edges, which is the so-called Li-Haldane conjecture. Thereafter, low-lying ES has been widely used as a fingerprint to investigate CFT and topology in highly entangled quantum matter [23–42].

However, most of the ES studies so far have focused on (quasi) 1D systems numerically, due to the exponential growth of computation complexity and memory cost. The existing numerical methods such as the exact diagonalization (ED) and the density matrix renormalization group (DMRG) have significant limitations for approaching large entangling region. We note that the quantum Monte Carlo (QMC) is a powerful tool for studying large size and higher dimensional open quantum many-body systems [43, 44], which has been developed to extract the entanglement spectral function combined with numerical analytic continuation [37–39, 45–56]. Though the method overcomes the exponential wall problem and can obtain large-scale entanglement spectral functions, it has rough precision and fails to distinguish the fine levels while the level structure always carries important information of CFT and topology. Moreover, the spectral function is also different from the full spectrum, which we will further compare to demonstrate that their character-

istics sometimes may be totally different. The other way to extract ES through QMC is to reconstruct it according to the knowledge of all integer Rényi entropies [57] because in principle, all the integer Rényi entropies can be calculated by QMC. The difficulty of this scheme is that the calculation of n -th Rényi entropy itself is not an easy task especially for higher n while the higher n -th entropy contains more information of low-lying levels.

Therefore, a practical scheme to extract fine low-lying ES with reduced computation complexity is urgent to be proposed. In this paper, we develop a protocol which can efficiently compute the ES via quantum Monte Carlo simulation for the entangling region with long boundaries and in higher dimensions. It can obtain fine low-lying levels of ES and is not limited to the freedom degree of the environment.

To demonstrate the strength of our method, a Heisenberg ladder in which we choose one chain as the entangling region has been investigated carefully. Compared with previous work studying the same system [20, 58, 59], we can not only address a much larger size with a ground-breaking record, but also clarify some misunderstandings in past work [20, 45] through our large-scale calculations. Furthermore, we calculate a 2D Heisenberg model to reveal the nontrivial continuous symmetry breaking phase using the structure of tower of states in the ES. We have to emphasize that our method is not limited to these particular systems, yet it can be widely applied to any models which can be simulated via QMC.

Method.- In a quantum many-body system, the ES of a subsystem (entangling region) A with the rest of the system B (environment) is constructed via the reduced density matrix (RDM), defined as the partial trace of the total density matrix ρ over a complete basis of B , i.e. $\rho_A = \text{Tr}_B(\rho)$. The RDM ρ_A can be interpreted as an effective thermodynamic density matrix $e^{-\mathcal{H}_A}$ through an entanglement Hamiltonian \mathcal{H}_A . The spectrum of the

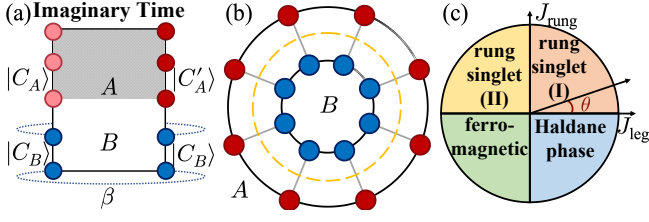


FIG. 1. (a) A path integral configuration of a reduced density matrix. The length of imaginary time is β , and the time boundary of B/A is periodic/open; (b) Lattice of the Spin-1/2 Heisenberg ladder from an overhead view, with spins in A and B depicted by red and blue circles respectively; (c) Its phase diagram by denoting $J_{\text{leg}} = \cos \theta$ and $J_{\text{rung}} = \sin \theta$.

entanglement Hamiltonian is usually denoted as the ES.

Due to the exponential growth of the computation complexity and the memory cost, it is intractable for the existing numerical methods such as the exact diagonalization (ED) and the density matrix renormalization group (DMRG) to approach entangling regions with long boundaries and higher dimensions. Because of the finite computer memory, these numerical methods are limited to short boundary only. Another way is to extract the low-lying entanglement spectrum (ES) through the quantum Monte Carlo simulation combined with stochastic analytic continuation (SAC), both in bosonic [45, 48, 60] and fermionic systems [37–39]. Especially in bosonic systems, the ES of spin ladders can be obtained even under a very long length $L = 100$ [45]. However, the ES obtained in this way can not show the fine levels but only the dispersion and weight of the spectral function. Nevertheless, the refined structure of ES, e.g., degeneracy, is important for identifying the CFT and topology.

The solution comes from QMC + ED: Tracing the environment via QMC and obtaining the exact low-lying levels through ED. The weight of RDM element $|C_A\rangle\langle C'_A|$ can be written in the path integral language as

$$\rho_{AC_A, C'_A} = \sum_{\{C_B\}} \langle C_A, C_B | e^{-\beta H} | C'_A, C_B \rangle, \quad \beta \rightarrow \infty, \quad (1)$$

where C_A , C'_A are the configurations of the RDM, and C_B is the configurations of environment B .

It can be treated as a general partition function under a special boundary condition along the imaginary time axis (see Fig. 1(a)), which is much more convenient to be simulated by quantum Monte Carlo (QMC). We deal with this special partition function in Eq. (1) in the framework of stochastic series expansion (SSE) method [61–65]. Of course it can be simulated by other path integral QMC [66–71]. The only difference compared with the normal SSE is that we open the boundary of the imaginary time in the region A and keep the periodic boundary condition to that of the environment B .

The value of each element in the RDM can be approached with the frequency of the samplings. It means

that the ρ_{AC_A, C'_A} is proportional to $N_{C_A, C'_A}/N_{\text{total}}$, where the N_{C_A, C'_A} is the amount of samplings that the upper/below imaginary time boundary configuration is C_A/C'_A and N_{total} is the total amount of samplings [72].

Example 1: Antiferromagnetic (AFM) Spin-1/2 Heisenberg Ladder.— To demonstrate the power of our method, we compute the ES of two-leg Heisenberg ladder with $L = 12, 16, 20, 24$ where the entangled boundary splits the ladder into two chains as shown in Fig. 1(b). The ES of this model has been carefully studied via ED for small sizes where $L = 10, 12, 14$ in previous work [20] and it has a well-known phase diagram (See Fig. 1(c)). The spins on the ladder are coupled through the nearest neighbor Heisenberg interactions, where J_{leg} denotes the intra-chain strength along the leg and J_{rung} denotes the inter-chain strength on the rung. We first simulate with $J_{\text{leg}} = 1$ and $J_{\text{rung}} = 1.732$ ($\theta = \pi/3$) at $\beta = 100$. The reason for this choice of parameters is that $\beta = 100$ ($T = J_{\text{leg}}/100$) is a temperature low enough for a gapped rung singlet (I) phase which has been studied with ED in Ref. [20], therefore it is convenient for us to compare the results.

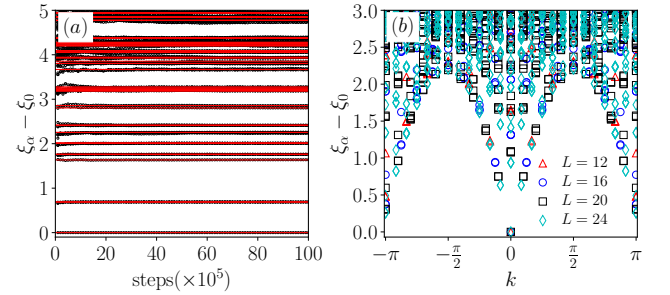


FIG. 2. (a) The comparison of low lying entanglement excitation spectra obtained by pure ED and QMC+ED with different Monte Carlo steps. The red lines are the results obtained by pure ED and the black dots are the results obtained by QMC+ED. Here we choose $L = 8$. (b) Entanglement excitation spectra versus total momenta k in the chain direction for $\theta = \pi/3$.

Firstly, we present a comparison of the spectrum obtained through QMC+ED and directly through ED with system size $L = 8$, as illustrated in Fig. 2(a). It is evident that the spectrum obtained via QMC+ED approaches that of ED as the sample size increases, and higher energy levels require a greater number of sampling iterations. It is easy to be understood because the QMC of course samples the lower energy configurations with heavier weight preferentially, thus the low-lying levels converge first.

After demonstrating the power of this method, we want to answer some physical questions. For example, there is a contradiction for the ES in the rung singlet (I) phase of the Heisenberg ladder in previous works [20, 45]. The ES here is expected to bear the low-energy CFT structure, i.e., the ground level of ES, ξ_0 , will scale as $\xi_0/L = e_0 +$

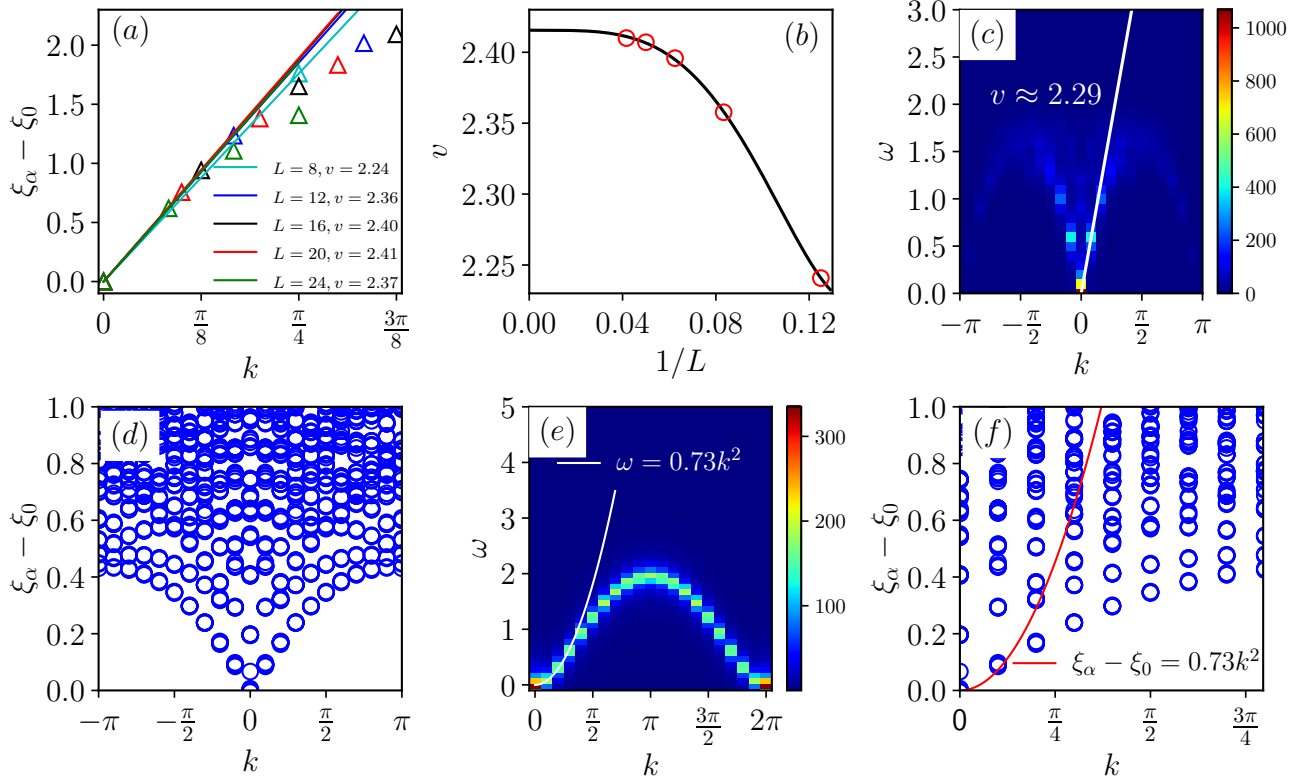


FIG. 3. (a) The fitting of velocity v according to the numerical results with different size. (b) The extrapolation of v with $1/L$. (c) Spectral function of the system with size $L = 24$ and its fitting of v . (d) Entanglement spectrum versus total momenta k in the chain direction for $\theta = 2\pi/3$. The system size is $L = 20$. (e) The entanglement spectral function of FM Heisenberg ladder with $L = 20$. Its quadratic fitting curve near the gapless point. (f) The quadratic fitting curve in the full entanglement spectrum.

$d_1/L^2 + \mathcal{O}(1/L^3)$ where the $d_1 = \pi cv/6$ according to the CFT prediction with the central charge $c = 1$ and v is the velocity of ES near the gapless point [20], i.e. the Cloiseaux-Pearson spectrum of the quantum spin chain, $v|\sin(k)|$ [73]. The fitting for the fine levels of the ES by ED at $L = 14$ (its largest size) gave $v \sim 2.36$ while the fitting for the rough spectral function of entanglement by QMC combined with SAC at $L = 100$ pointed to a double value $v \sim 4.58$ [45]. Therefore, the later one thought it is because the finite size effect of ES is serious. Since our method avoids the limitation of the environment size, we can calculate larger sizes to see how the v scales with L . If the ES has obvious finite size effect, the v certainly will increase following the size. In Fig. 2(b), we give the the low-lying levels of ES in different sizes which is much larger than the pure ED's results, so that we can inspect the finite size effect here.

The spectra of the system with various system sizes obtained by QMC+ED is shown in Fig. 2(b), and the results are consistent with the ED results show in Ref. [20]. In the Fig. 3(a), we fit the velocities of different sizes via linear functions. All the lines are close to each other,

representing that their velocities are similar. Furthermore, we draw a fitting line for the velocity v of different size L in Fig. 3(b), which scales to a value in the region $[2.40, 2.45]$ at infinite size. It turns out that the velocity is almost unchanged with size L and convergent to ~ 2.41 , which is inconsistent to the result of spectral function by QMC+SAC where $v \sim 4.58$.

In order to show the spectral property of the system and avoid the difference between the ES and entanglement spectral function, we also calculate the spectral function of entanglement. For a physical observable denoted by \mathcal{O} , the spectral function $S(\omega)$ can be written as

$$S(\omega) = \frac{1}{\pi} \sum_{m,n} e^{-\beta E_n} |\langle n | \mathcal{O} | m \rangle|^2 \delta(\omega - [E_m - E_n]), \quad (2)$$

where $\{|n\rangle\}$ and $\{E_n\}$ are the eigenstates and eigenvalues of the Hamiltonian \mathcal{H} respectively. In the following, we choose \mathcal{O} as the spin operator S^z , $|m\rangle$ as the ground state, and E_m as the ground state energy. The choice is same as the Ref. [45] which is convenient for comparisons.

Fig. 3(c) shows the spectral function of the system with

size $L = 24$ and we also give the velocity $v \sim 2.29$. It reveals that the contradiction between the ES and entanglement spectral function is not because of the difference of the definition. We favor the reason that the settings of some constant are different between the two Refs. [20, 45]

Example 2: Ferromagnetic (FM) Spin-1/2 Heisenberg Ladder.- Furthermore, we simulate the case with ferromagnetic $J_{\text{leg}} = -1$ and antiferromagnetic $J_{\text{rung}} = 1.732$ at $\beta = 100$ on the two-leg Heisenberg ladder for $L = 8, 12, 16, 20$ and compare the results with that in Ref. [20], in which case the ladder is in the gapped rung singlet (II) phase.

According to Refs. [45, 74–76], the lowest-energy excitations at $k = 2\pi/L$ corresponds to the one magnon state and behaves as $E = 2J_{\text{eff}}\sin^2(k/2)$, where J_{eff} is an effective chain coupling. The results in Ref. [20] did not show the quadratic behavior due to the small system size. Other studies explained this non-quadratic dispersion via long-range boundary Hamiltonian [22, 58, 59]. Meanwhile, the QMC+SAC simulation at $L = 100$ in the Ref. [45] shows the spectral function of entanglement is indeed a quadratic dispersion, which further demonstrated the finite size effect of ES here.

In order to check whether the loss of quadratic dispersion is because of the finite size effect, we further try to calculate the ES and its spectral function for larger sizes. Fig. 3(d) shows the results with $L = 20$, in which there is no obvious quadratic dispersion near $k = 0$. Actually, we haven't seen an obvious change of the dispersion from the linear to the quadratic when increasing the size.

In fact, the answer of the contradiction comes from the difference between the ES and entanglement spectral function instead of the finite size effect. The results of the FM Heisenberg ladder indicates that the spectrum and spectral function exhibit distinct behaviors at low energy levels. As it is shown in Fig. 3(e), the ES in $L = 20$ does not show a quadratic dispersion while the spectral function does. We try to draw the curve of the spectral function in the ES levels as shown in Fig. 3(f), which further demonstrates that the spectral function goes up quickly beyond the lowest levels of ES. Thus, the spectral function is not the descender line of full spectrum at all in this FM case which is opposite to the AFM case. This is actually the intrinsic reason that the FM ES has no quadratic dispersion. It also answers that why the top of the entanglement spectral function [45] is much larger than the top of the descender line of ES [20].

Two dimensional examples.- We then calculate a periodic boundary condition (PBC) 20×20 square lattice AFM Heisenberg model with two different cut-geometries of A . If we choose the A as a chain as the yellow dots (A region) in Fig. 4(a) displays, it presents a linear dispersion ES reflecting the Néel order of this AFM model, as shown in Fig. 4(b). What's more, the linear low-lying levels is the famous tower of states (TOS) structure which reveals the continuous symmetry breaking here [22, 77–

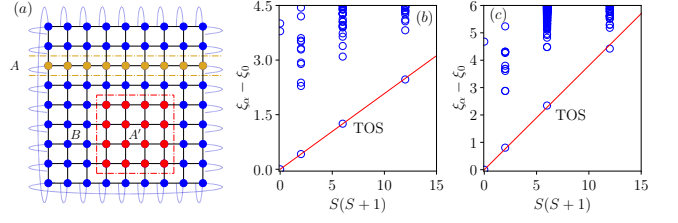


FIG. 4. (a) The AFM Heisenberg model on the square lattice. The dashed lines are to illustrate the bipartition into two subsystems. The yellow dashed lines illustrate the cutting method that A is a ring and the red dashed lines illustrate the method that A' is a block. For each cutting method, the other part is denoted as B . We consider the square lattice model with size 20×20 . We show the entanglement spectrum of EH corresponding to (b) A with length $L = 20$ and (c) A' with size 4×4 . The TOS levels are connected by a red line. All the data are calculated in the total $S^z = 0$ sector.

79]. Meanwhile, if we set A as a 4×4 region as the red dots (A' region) in Fig. 4(a), the ES also shows a TOS character as shown in Fig. 4(c). Usually, the TOS holds in cornerless cutting cases, this is the first evidence supporting the TOS also arises in cornered cutting.

The advantage and disadvantage of this method.- We have to emphasize that the computational complexity of this method is exponential/polynomial for the freedom degree of A/B . Since we trace all the freedom degrees of B and sample them, the complexity of B part is as same as the normal QMC which increases in the power-law. At the same time, we sample all the freedom degree of A without any trace operation, thus its complexity is proportional to the dimension of the RDM, which is exponentially increasing. Therefore, the advantage of this method is that it is basically not limited to the size of the environment and can obtain the RDM and fine levels of the ES.

However, because the important information is always contained in the low-lying ES, while the importance sampling of QMC just presents the low-lying levels first, actually we can set a cut-off for the sampling to avoid the additional cost for high levels. For example, if we only consider the first excited gap of the ES (the Schmidt gap[80, 81]), the sampling amount could be small. As shown in the Fig. 2(a), the first gap converges very quickly over the Monte Carlo sampling.

To compare with ED, this method can obtain ρ_A in a much larger size. To compare with the QMC+SAC scheme, it is not limited to the cut-geometry between A and B , and it can extract the fine levels of low-lying ES [82]. Similarly, although the Bisognano-Wichmann theorem gives the detailed form of entanglement Hamiltonian, it holds under some strict conditions (e.g., the entanglement region has no corner, the original Hamiltonian satisfies translation symmetry) and may lose the effectiveness in many lattice models [83–86].

Conclusions and outlooks.- We propose a practical scheme to extract the fine levels of entanglement spectrum from the method of quantum Monte Carlo simulation combined with exact diagonalization. It can extract the fine information of low-lying ES for large-scale quantum many-body systems whose environment has huge degrees of freedom. Using this method, we answer the previous contradiction for the entanglement spectrum in a Heisenberg ladder system. Furthermore, we calculate the ES of a 2D AFM Heisenberg model within two different cut-geometries. Both the cornered and cornerless cases show the TOS character which reflects the continuous symmetry breaking here.

In summary, the reduced density matrix can be obtained in larger size via QMC within this frame. Therefore, other observables such as von Neumann entropy and off-diagonal measurements can also be extracted in this way.

Acknowledgement.- We would like to thank Wei Zhu, Yin Tang, Xue-Feng Zhang, Shangqiang Ning and Han-Qing Wu for fruitful discussions. We acknowledge the start-up funding of Westlake University. The authors also acknowledge Beijing PARATERA Tech Co.,Ltd.(<https://www.paratera.com/>) for providing HPC resources that have contributed to the research results reported within this paper.

* zhengyan@westlake.edu.cn

- [1] Luigi Amico, Rosario Fazio, Andreas Osterloh, and Vlatko Vedral, “Entanglement in many-body systems,” *Rev. Mod. Phys.* **80**, 517–576 (2008).
- [2] Nicolas Laflorencie, “Quantum entanglement in condensed matter systems,” *Physics Reports* **646**, 1–59 (2016), quantum entanglement in condensed matter systems.
- [3] G. Vidal, J. I. Latorre, E. Rico, and A. Kitaev, “Entanglement in quantum critical phenomena,” *Phys. Rev. Lett.* **90**, 227902 (2003).
- [4] V. E. Korepin, “Universality of entropy scaling in one dimensional gapless models,” *Phys. Rev. Lett.* **92**, 096402 (2004).
- [5] Alexei Kitaev and John Preskill, “Topological entanglement entropy,” *Phys. Rev. Lett.* **96**, 110404 (2006).
- [6] Michael Levin and Xiao-Gang Wen, “Detecting topological order in a ground state wave function,” *Phys. Rev. Lett.* **96**, 110405 (2006).
- [7] Pasquale Calabrese and Alexandre Lefevre, “Entanglement spectrum in one-dimensional systems,” *Phys. Rev. A* **78**, 032329 (2008).
- [8] Eduardo Fradkin and Joel E. Moore, “Entanglement entropy of 2d conformal quantum critical points: Hearing the shape of a quantum drum,” *Phys. Rev. Lett.* **97**, 050404 (2006).
- [9] Zohar Nussinov and Gerardo Ortiz, “Sufficient symmetry conditions for Topological Quantum Order,” *Proc. Nat. Acad. Sci.* **106**, 16944–16949 (2009).
- [10] Zohar Nussinov and Gerardo Ortiz, “A symmetry principle for topological quantum order,” *Annals Phys.* **324**, 977–1057 (2009).
- [11] H. Casini and M. Huerta, “Universal terms for the entanglement entropy in 2+1 dimensions,” *Nuclear Physics B* **764**, 183–201 (2007).
- [12] Wenjie Ji and Xiao-Gang Wen, “Noninvertible anomalies and mapping-class-group transformation of anomalous partition functions,” *Phys. Rev. Research* **1**, 033054 (2019).
- [13] Wenjie Ji and Xiao-Gang Wen, “Categorical symmetry and noninvertible anomaly in symmetry-breaking and topological phase transitions,” *Phys. Rev. Research* **2**, 033417 (2020).
- [14] Liang Kong, Tian Lan, Xiao-Gang Wen, Zhi-Hao Zhang, and Hao Zheng, “Algebraic higher symmetry and categorical symmetry: A holographic and entanglement view of symmetry,” *Phys. Rev. Research* **2**, 043086 (2020).
- [15] Xiao-Chuan Wu, Wenjie Ji, and Cenke Xu, “Categorical symmetries at criticality,” *Journal of Statistical Mechanics: Theory and Experiment* **2021**, 073101 (2021).
- [16] Jiarui Zhao, Zheng Yan, Meng Cheng, and Zi Yang Meng, “Higher-form symmetry breaking at ising transitions,” *Phys. Rev. Research* **3**, 033024 (2021).
- [17] Xiao-Chuan Wu, Chao-Ming Jian, and Cenke Xu, “Universal Features of Higher-Form Symmetries at Phase Transitions,” *SciPost Phys.* **11**, 33 (2021).
- [18] Hui Li and F. D. M. Haldane, “Entanglement spectrum as a generalization of entanglement entropy: Identification of topological order in non-abelian fractional quantum hall effect states,” *Phys. Rev. Lett.* **101**, 010504 (2008).
- [19] Ronny Thomale, D. P. Arovas, and B. Andrei Bernevig, “Nonlocal order in gapless systems: Entanglement spectrum in spin chains,” *Phys. Rev. Lett.* **105**, 116805 (2010).
- [20] Didier Poilblanc, “Entanglement spectra of quantum heisenberg ladders,” *Phys. Rev. Lett.* **105**, 077202 (2010).
- [21] John Schliemann and Andreas M Läuchli, “Entanglement spectra of heisenberg ladders of higher spin,” *Journal of Statistical Mechanics: Theory and Experiment* **2012**, P11021 (2012).
- [22] Nicolas Laflorencie, “Quantum entanglement in condensed matter systems,” *Physics Reports* **646**, 1–59 (2016).
- [23] Frank Pollmann, Ari M. Turner, Erez Berg, and Masaki Oshikawa, “Entanglement spectrum of a topological phase in one dimension,” *Phys. Rev. B* **81**, 064439 (2010).
- [24] Lukasz Fidkowski, “Entanglement spectrum of topological insulators and superconductors,” *Phys. Rev. Lett.* **104**, 130502 (2010).
- [25] Hong Yao and Xiao-Liang Qi, “Entanglement entropy and entanglement spectrum of the kitaev model,” *Phys. Rev. Lett.* **105**, 080501 (2010).
- [26] Xiao-Liang Qi, Hosho Katsura, and Andreas W. W. Ludwig, “General relationship between the entanglement spectrum and the edge state spectrum of topological quantum states,” *Phys. Rev. Lett.* **108**, 196402 (2012).
- [27] Elena Canovi, Elisa Ercolessi, Piero Naldesi, Luca Taddea, and Davide Vodola, “Dynamics of entanglement entropy and entanglement spectrum crossing a quantum phase transition,” *Phys. Rev. B* **89**, 104303 (2014).
- [28] David J. Luitz, Fabien Alet, and Nicolas Laflorencie, “Universal behavior beyond multifractality in quantum many-body systems,” *Phys. Rev. Lett.* **112**, 057203 (2014).

- (2014).
- [29] David J. Luitz, Fabien Alet, and Nicolas Laflorencie, “Shannon-rényi entropies and participation spectra across three-dimensional $o(3)$ criticality,” *Phys. Rev. B* **89**, 165106 (2014).
 - [30] David J Luitz, Nicolas Laflorencie, and Fabien Alet, “Participation spectroscopy and entanglement hamiltonian of quantum spin models,” *Journal of Statistical Mechanics: Theory and Experiment* **2014**, P08007 (2014).
 - [31] Chia-Min Chung, Lars Bonnes, Pochung Chen, and Andreas M. Läuchli, “Entanglement spectroscopy using quantum monte carlo,” *Phys. Rev. B* **89**, 195147 (2014).
 - [32] Hannes Pichler, Guanyu Zhu, Alireza Seif, Peter Zoller, and Mohammad Hafezi, “Measurement protocol for the entanglement spectrum of cold atoms,” *Phys. Rev. X* **6**, 041033 (2016).
 - [33] J. Ignacio Cirac, Didier Poilblanc, Norbert Schuch, and Frank Verstraete, “Entanglement spectrum and boundary theories with projected entangled-pair states,” *Phys. Rev. B* **83**, 245134 (2011).
 - [34] Vladimir M. Stojanović, “Entanglement-spectrum characterization of ground-state nonanalyticities in coupled excitation-phonon models,” *Phys. Rev. B* **101**, 134301 (2020).
 - [35] Wu-zhong Guo, “Entanglement spectrum of geometric states,” *Journal of High Energy Physics* **2021**, 1–33 (2021).
 - [36] Tarun Grover, “Entanglement of interacting fermions in quantum monte carlo calculations,” *Phys. Rev. Lett.* **111**, 130402 (2013).
 - [37] Fakher F. Assaad, Thomas C. Lang, and Francesco Parisen Toldin, “Entanglement spectra of interacting fermions in quantum monte carlo simulations,” *Phys. Rev. B* **89**, 125121 (2014).
 - [38] Fakher F. Assaad, “Stable quantum monte carlo simulations for entanglement spectra of interacting fermions,” *Phys. Rev. B* **91**, 125146 (2015).
 - [39] Francesco Parisen Toldin and Fakher F. Assaad, “Entanglement hamiltonian of interacting fermionic models,” *Phys. Rev. Lett.* **121**, 200602 (2018).
 - [40] Xue-Jia Yu, Rui-Zhen Huang, Hong-Hao Song, Limei Xu, Chengxiang Ding, and Long Zhang, “Conformal boundary conditions of symmetry-enriched quantum critical spin chains,” *Phys. Rev. Lett.* **129**, 210601 (2022).
 - [41] Gergo Roósz and Carsten Timm, “Entanglement of electrons and lattice in a luttinger system,” *Phys. Rev. B* **104**, 035405 (2021).
 - [42] Gergo Roósz and Karsten Held, “Density matrix of electrons coupled to einstein phonons and the electron-phonon entanglement content of excited states,” *Phys. Rev. B* **106**, 195404 (2022).
 - [43] Zi Cai, Ulrich Schollwöck, and Lode Pollet, “Identifying a bath-induced bose liquid in interacting spin-boson models,” *Phys. Rev. Lett.* **113**, 260403 (2014).
 - [44] Zheng Yan, Lode Pollet, Jie Lou, Xiaoqun Wang, Yan Chen, and Zi Cai, “Interacting lattice systems with quantum dissipation: A quantum monte carlo study,” *Phys. Rev. B* **97**, 035148 (2018).
 - [45] Zheng Yan and Zi Yang Meng, “Unlocking the general relationship between energy and entanglement spectra via the wormhole effect,” *Nature Communications* **14**, 2360 (2023).
 - [46] Siying Wu, Xiaoxue Ran, Binbin Yin, Qi-Fang Li, Bin-Bin Mao, Yan-Cheng Wang, and Zheng Yan, “Classical model emerges in quantum entanglement: Quantum monte carlo study for an ising-heisenberg bilayer,” *Phys. Rev. B* **107**, 155121 (2023).
 - [47] Menghan Song, Jiarui Zhao, Zheng Yan, and Zi Yang Meng, “Different temperature dependence for the edge and bulk of the entanglement hamiltonian,” *Phys. Rev. B* **108**, 075114 (2023).
 - [48] Zenan Liu, Rui-Zhen Huang, Zheng Yan, and Dao-Xin Yao, “Probing li-haldane conjecture with a perturbed boundary,” (2023), arXiv:2303.00772 [cond-mat.str-el].
 - [49] Hui Shao and Anders W. Sandvik, “Progress on stochastic analytic continuation of quantum monte carlo data,” *Physics Reports* **1003**, 1–88 (2023).
 - [50] Anders W. Sandvik, “Stochastic method for analytic continuation of quantum monte carlo data,” *Phys. Rev. B* **57**, 10287–10290 (1998).
 - [51] K. S. D. Beach, “Identifying the maximum entropy method as a special limit of stochastic analytic continuation,” arXiv e-prints , cond-mat/0403055 (2004), arXiv:cond-mat/0403055 [cond-mat.str-el].
 - [52] Anders W. Sandvik, “Constrained sampling method for analytic continuation,” *Phys. Rev. E* **94**, 063308 (2016).
 - [53] Olav F. Syljuåsen, “Using the average spectrum method to extract dynamics from quantum monte carlo simulations,” *Phys. Rev. B* **78**, 174429 (2008).
 - [54] Hui Shao, Yan Qi Qin, Sylvain Capponi, Stefano Chesi, Zi Yang Meng, and Anders W. Sandvik, “Nearly deconfined spinon excitations in the square-lattice spin-1/2 heisenberg antiferromagnet,” *Phys. Rev. X* **7**, 041072 (2017).
 - [55] Zheng Yan, Yan-Cheng Wang, Nvsn Ma, Yang Qi, and Zi Yang Meng, “Topological phase transition and single/multi anyon dynamics of Z_2 spin liquid,” *npj Quantum Mater.* , 39 (2021).
 - [56] Chengkang Zhou, Zheng Yan, Han-Qing Wu, Kai Sun, Oleg A. Starykh, and Zi Yang Meng, “Amplitude mode in quantum magnets via dimensional crossover,” *Phys. Rev. Lett.* **126**, 227201 (2021).
 - [57] Chia-Min Chung, Lars Bonnes, Pochung Chen, and Andreas M. Läuchli, “Entanglement spectroscopy using quantum monte carlo,” *Phys. Rev. B* **89**, 195147 (2014).
 - [58] Andreas M. Läuchli and John Schliemann, “Entanglement spectra of coupled $s = \frac{1}{2}$ spin chains in a ladder geometry,” *Phys. Rev. B* **85**, 054403 (2012).
 - [59] J. Ignacio Cirac, Didier Poilblanc, Norbert Schuch, and Frank Verstraete, “Entanglement spectrum and boundary theories with projected entangled-pair states,” *Phys. Rev. B* **83**, 245134 (2011).
 - [60] Chuha Li, Rui-Zhen Huang, Yi-Ming Ding, Zi Yang Meng, Yan-Cheng Wang, and Zheng Yan, “Relevant long-range interaction of the entanglement hamiltonian emerges from a short-range system,” (2023), arXiv:2309.16089 [cond-mat.str-el].
 - [61] Anders W. Sandvik and Juhani Kurkijärvi, “Quantum Monte Carlo simulation method for spin systems,” *Phys. Rev. B* **43**, 5950–5961 (1991).
 - [62] Anders W. Sandvik, “Stochastic series expansion method with operator-loop update,” *Phys. Rev. B* **59**, R14157–R14160 (1999).
 - [63] Olav F. Syljuåsen and Anders W. Sandvik, “Quantum monte carlo with directed loops,” *Phys. Rev. E* **66**, 046701 (2002).
 - [64] Zheng Yan, Yongzheng Wu, Chenrong Liu, Olav F. Syljuåsen, Jie Lou, and Yan Chen, “Sweeping cluster

- algorithm for quantum spin systems with strong geometric restrictions,” *Phys. Rev. B* **99**, 165135 (2019).
- [65] Zheng Yan, “Global scheme of sweeping cluster algorithm to sample among topological sectors,” *Phys. Rev. B* **105**, 184432 (2022).
- [66] Masuo Suzuki, Seiji Miyashita, and Akira Kuroda, “Monte carlo simulation of quantum spin systems. i,” *Progress of Theoretical Physics* **58**, 1377–1387 (1977).
- [67] J. E. Hirsch, R. L. Sugar, D. J. Scalapino, and R. Blankenbecler, “Monte carlo simulations of one-dimensional fermion systems,” *Phys. Rev. B* **26**, 5033–5055 (1982).
- [68] Masuo Suzuki, “Relationship between d-dimensional quantal spin systems and (d+ 1)-dimensional ising systems: Equivalence, critical exponents and systematic approximants of the partition function and spin correlations,” *Progress of theoretical physics* **56**, 1454–1469 (1976).
- [69] Henk W. J. Blöte and Youjin Deng, “Cluster monte carlo simulation of the transverse ising model,” *Phys. Rev. E* **66**, 066110 (2002).
- [70] Chun-Jiong Huang, Longxiang Liu, Yi Jiang, and Youjin Deng, “Worm-algorithm-type simulation of the quantum transverse-field ising model,” *Physical Review B* **102**, 094101 (2020).
- [71] Zhijie Fan, Chao Zhang, and Youjin Deng, “Clock factorized quantum monte carlo method for long-range interacting systems,” (2023), arXiv:2305.14082 [physics.comp-ph].
- [72] It’s worth noting that the sign should be considered if the weight is not positive.
- [73] Jacques des Cloizeaux and J. J. Pearson, “Spin-wave spectrum of the antiferromagnetic linear chain,” *Phys. Rev.* **128**, 2131–2135 (1962).
- [74] Bethe H., “Zur theorie der metalle,” *Z. Physik* **71**, 205–226 (1931).
- [75] H C Fogedby, “The spectrum of the continuous isotropic quantum heisenberg chain: quantum solitons as magnon bound states,” *Journal of Physics C: Solid State Physics* **13**, L195–L200 (1980).
- [76] F D M Haldane, “Excitation spectrum of a generalised heisenberg ferromagnetic spin chain with arbitrary spin,” *Journal of Physics C: Solid State Physics* **15**, L1309–L1313 (1982).
- [77] F. Kolley, S. Depenbrock, I. P. McCulloch, U. Schollwöck, and V. Alba, “Entanglement spectroscopy of su(2)-broken phases in two dimensions,” *Phys. Rev. B* **88**, 144426 (2013).
- [78] Vincenzo Alba, Masudul Haque, and Andreas M. Läuchli, “Entanglement spectrum of the two-dimensional bose-hubbard model,” *Phys. Rev. Lett.* **110**, 260403 (2013).
- [79] Alexander Wietek, Michael Schuler, and Andreas M Läuchli, “Studying continuous symmetry breaking using energy level spectroscopy,” arXiv preprint arXiv:1704.08622 (2017).
- [80] Abolfazl Bayat, Henrik Johannesson, Sougato Bose, and Pasquale Sodano, “An order parameter for impurity systems at quantum criticality,” *Nature communications* **5**, 3784 (2014).
- [81] Johnnie Gray, Sougato Bose, and Abolfazl Bayat, “Many-body localization transition: Schmidt gap, entanglement length, and scaling,” *Phys. Rev. B* **97**, 201105 (2018).
- [82] In the QMC+SAC method, because the spectral function is gained from the imaginary time correlation function via numerical analytic continuation, it requires that A should have periodic boundary condition to guarantee a well-defined momentum k . In other words, the analytic continuation depends closely on the cut form of the entanglement. However, our method can study any geometry for the A .
- [83] Marcello Dalmonte, Viktor Eisler, Marco Falconi, and Benoît Vermersch, “Entanglement hamiltonians: From field theory to lattice models and experiments,” *Annalen der Physik* **11**, n–a (2022).
- [84] T Mendes-Santos, G Giudici, M Dalmonte, and MA Rajabpour, “Entanglement hamiltonian of quantum critical chains and conformal field theories,” *Physical Review B* **100**, 155122 (2019).
- [85] T Mendes-Santos, G Giudici, R Fazio, and M Dalmonte, “Measuring von neumann entanglement entropies without wave functions,” *New Journal of Physics* **22**, 013044 (2020).
- [86] G Giudici, T Mendes-Santos, and P Calabrese, “Entanglement hamiltonians of lattice models via the bisognanowichmann theorem,” *Physical Review B* **98**, 134403 (2018).